ISSN: 2456-9348
Vol (01) _Issue (04) Impact Factor: 4.520

iJETRM
International Journal of Engineering Technology Research & Management

NUMERICAL SIMULATION OF HEAT TRANSFER CHARACTERISTICS OF COMBINED ELECTROOSMOTIC AND PRESSURE-DRIVEN FULLY-DEVELOPED FLOW OF POWER-LAW FLUIDS IN MICROTUBES

Tikendra Nath Verma[*1]
Prerana Nashine [2]
Thokchom Subhaschandra Singh[3]
Moon Banerjee[4]
[*1]Department of Mechanical Engineering, National Institute of Technology Manipur-795004, India
[2]Department of Mechanical Engineering, National Institute of Technology Rourkela-769008, India
[3]Department of Mechanical Engineering, National Institute of Technology Manipur-795004, India
[4]Department of Mechanical Engineering, Amity University, Gwalior, MP-474001, India
*Corresponding author: verma.tikks@gmail.com; tikendra.me@nitmanipur.ac.in
Ph: **+91-98271-83393**

Abstract

Thermal transport characteristics of electro-osmotic flow of non-Newtonian (power-law) fluids through microtube have been studied. Non-Newtonian properties of the fluids can influence the thermal behaviour of the flow by affecting the rate of heat convection through viscous dissipation. Electroosmotic phenomenon affects the heat transfer rate through a heat generation process because of the fluid's resistivity, known as Joule heating. A complete parametric study has been carried out to investigate the effect of different thermo-physical parameters on the thermal behavior of the flow. The governing equations have been solved analytically and by numerical methods under constant wall heat flux condition taking into account the effects of viscous dissipation and Joule heating. Power-law fluids of both shear-thinning and shear-thickening nature have been considered. The governing equations have been solved only for hydro dynamically and thermally fully-developed flow.

Keywords: -Micro tube, Electroosmotic Flow, Pressure-Driven, Viscous Dissipation, Joule Heating, Non-Newtonian (Power-Law) Fluid, Electric Double Layer

Introduction

The increasing interest in the area of microscale heat transfer can be attributed mainly to the miniaturization of electronic components. Fluid flow through microstructures can be efficiently achieved using an appropriate pumping system. Of the available mechanisms, electroosmotic pumps have been found feasible for a wide variety of applications, owing to their simple design and easier fabrication due to the absence of moving components. Precise flow control can also be achieved in these pumps. In the electroosmotic phenomenon, [1] bulk

iJETRM
International Journal of Engineering Technology Research & Management

motion of the ions and thus the fluid, can be achieved by applying external electric field along the microtube axis. The electroosmotic force is a form of body force.

The interaction between the solid surface and the electrolytic solution was discovered by Reuss[2]. According to him, a relative electrostatic charge is formed on the inner wall of the microtube. This is known as zeta potential. Counter ions are attracted to the charged surface and a counter-ion rich layer is formed in the fluid, called electric double layer (EDL). The electric potential distribution can be determined using the Poisson's equation. A rapid decrease in the potential is seen with increasing distance from the microtube surface. The EDL thickness is characterized by the Debye length which is the distance from the charged surface where the potential is 37% of the zeta potential. Presence of a pressure field, due to an alternate pumping mechanism or variations in zeta potential, changes the velocity profile of the flow.

Burgreen and Nakache[3] carried out research on the electroosmotic flow dynamics at a primary level for slit capillaries and Rice and Whitehead for cylindrical capillaries, at low zeta potentials. This was extended for higher zeta potentials by Levine et al.[4]. Flow characteristics of fully-developed flow in rectangular microchannel were numerically studies by Arulanandam and Li [5]. Xuan and Li [6] designed a methodology to determine flow profiles for electrokinetic flow in microchannels of arbitrary geometry and wall charge distribution. Electroosmotic phenomenon causes the fluid to heat up because of the fluid's electrical resistivity to the applied electric field. This is called Joule heating.

Maynes and Webb [7] were the first to consider the thermal aspects of electroosmotic flow, analytically studying the convective transport for a parallel plate microchannel and circular microtube under constant heat flux and constant wall temperature condition for fully-developed region. This work was extended to higher zeta potential conditions by Liechty et al. [8]

Mathematical Formulation

In the present study, the flow of non-Newtonian (power law) electrolytic solution is considered for hydro dynamically and thermally developed conditions.

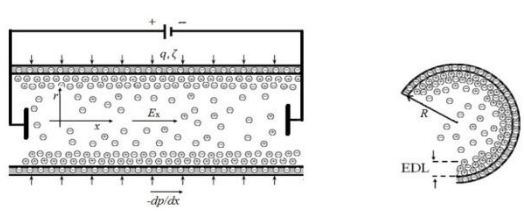

Fig.1.1 Schematic diagram of the problem illustrating the coordinate system, parameters driving the flow and the EDL.

The flow occurs under combined action of electro-osmotic force and pressure gradient. The microtube is in horizontal configuration with its radius being *R*. The geometry of the problem is depicted in Figure 1.

It is assumed that the charge in the EDL follows the Boltzmann distribution, which happens in the case of fully dissociated symmetric salt. The electric potential distribution is found by solving Poisson's equation [10]:

iJETRM
International Journal of Engineering Technology Research & Management

$$\nabla^2\varphi = -\frac{\rho_e}{\varepsilon} \tag{1}$$

Here ρ_e is the net electric charge density and $\varepsilon$is the fluid electric permittivity. The potential φ is a combination of externally imposed field, Φ and the EDL potential distribution in the solution, ψ. For an ideal solution of fully dissociated symmetric salt, the electric charge density is given by [10]

$$\rho_e = -2n_0 ez \sinh\left(\frac{ez\psi}{k_B T}\right) \tag{2}$$

where n_0 is the number ion concentration of neutral liquid, e is the charge of proton, z is the valence number of ions in the solution, k_B is the Boltzmann constant and T is the absolute temperature at a particular location.

In a fully-developed flow, since the electroosmotic potential varies only in r-direction and external potential varies only in x-direction, Eq.(1) becomes

$$\frac{1}{r}\frac{d}{dr}\left(r\frac{d\psi}{dr}\right) = \frac{2n_0 ez}{\varepsilon}\sinh\left(\frac{ez\psi}{k_B T}\right) \tag{3}$$

Since the temperature distribution does not affect the potential distribution much [11], the potential field and charge density can be calculated on the basis of an average temperature.

$$\frac{1}{r}\frac{d}{dr}\left(r\frac{d\psi}{dr}\right) = \frac{2n_0 ez}{\varepsilon}\sinh\left(\frac{ez\psi}{k_B T_{av}}\right) \tag{4}$$

In the non-dimensional form, the Eq.(4) becomes

$$\frac{d^2\psi^*}{dr^{*2}} + \frac{1}{r^*}\frac{d\psi^*}{dr^*} = \frac{2n_0 e^2 z^2}{\varepsilon k_B T_{av}} R^2 \sinh(\psi^*) \tag{5}$$

where $\psi^* = \frac{ez\psi}{k_B T_{av}}$, $r^* = \frac{r}{R}$ and $\left(\frac{2n_0 e^2 z^2}{\varepsilon k_B T_{av}}\right)^{-1/2}$ is called the Debye length, denoted by λ_D.

The dimensionless Debye-Hückel parameter can be defined as $K = {}^{\lambda_D}/_{R}$ So Eq. (5) becomes

$$\frac{d^2\psi^*}{dr^{*2}} + \frac{1}{r^*}\frac{d\psi^*}{dr^*} - K^2 \sinh(\psi^*) = 0 \tag{6}$$

The boundary conditions applicable are

$$\psi^*|_{r^*=1} = \zeta^* \text{and} \left.\frac{d\psi^*}{dr^*}\right|_{r^*=0} = 0 \tag{7}$$

where $\zeta^* = \frac{ez\zeta}{k_B T_B}$ is the dimensionless zeta potential.

The flow field of the non-Newtonian aqueous electrolyte is governed by continuity and Cauchy momentum equations. The continuity equation in the reduced form considering steady, incompressible and fully-developed flow is

$$\frac{du}{dx} = 0 \tag{8}$$

This is because, in fully-developed condition u is a function of r alone and velocity in the r-direction is considered to be zero. The Cauchy momentum equation in the x-direction becomes

$$\rho\frac{D\mathbf{V}}{Dt} = -\nabla p + \nabla.\boldsymbol{\tau} + \mathbf{F} \tag{9}$$

V is the velocity vector, p the applied pressure, $\boldsymbol{\tau}$ the stress tensor and **F** is the body force. Here, the body force is due to the applied electric field and is given by $\rho_e E_x$, where $E_x=-d\Phi/dx$ is the electric field acting in the x-direction. The body force also is assumed to act only in the x-direction as the electric field is assumed to act in that direction only. Since velocity variation is in r-direction alone, the stress tensor becomes $\mu\frac{du}{dr}$, where μ is the effective viscosity and given by

ISSN: 2456-9348
Vol (01) _Issue (04) Impact Factor: 4.520

iJETRM
International Journal of Engineering Technology Research & Management

$$\mu = \mu_0 \left[\left(\frac{du}{dr} \right)^2 \right]^{\frac{n-1}{2}} \tag{10}$$

where μ_0 is the consistency index, and n is the flow behavior index. n< 1 for shear thinning fluids, n = 1 for Newtonian fluids and n< 1 for shear thickening fluids.
Applying the expressions for the terms of the momentum equation as obtained above, Eq.(9) becomes

$$\frac{1}{r}\frac{d}{dr}\left\{ \mu_0 \left[\left(\frac{du}{dr} \right)^2 \right]^{\frac{n-1}{2}} \frac{du}{dr} \right\} = \frac{dp}{dx} + 2E_x n_0 ez \sinh\left(\frac{ez\psi}{k_B T_{av}} \right) \tag{11}$$

To non-dimensionalize the above equation, a reference velocity has to be considered. The Helmholtz-Smoluchowski electroosmotic velocity, u_{HS} , [9] has been taken as the reference velocity, which is given by

$$u_{HS} = n\lambda_D^{\frac{n-1}{n}} \left(-\frac{\varepsilon\zeta E_x}{\mu_0} \right)^{\frac{1}{n}} \tag{12}$$

and $u_{HS}$is the maximum possible electroosmotic velocity that can obtained when Debye-Hückel linearization is applied. Another velocity $u_{PD}$is considered which is the maximum velocity of pressure driven flow without electro kinetic effect.

$$u_{PD}^n = \left(\frac{n}{n+1} \right)^n \left(-\frac{1}{\mu_0}\frac{dp}{dx} R^{n+1} \right) \tag{13}$$

The non-dimensional velocity u^* is given by $u^*=u/u_{HS}$. By differentiating and reducing, the left hand side of Eq.(11) can be converted to the form $nN(r^*)\frac{d^2u}{dr^2}$ where $N(r^*) = \left[\left(\frac{du^*}{dr^*} \right)^2 \right]^{\frac{n-1}{2}}$. Therefore, the dimensionless momentum equation becomes

$$nN(r^*)\left\{ \frac{1}{nr^*}\frac{du^*}{dr^*} + \frac{d^2u^*}{dr^{*2}} \right\} = -\left(\frac{n+1}{n} \right)^n \Gamma - \frac{K^{n+1}}{n^n \zeta^*} \sinh\psi^* \tag{14}$$

where $\Gamma = \frac{u_{PD}^n}{u_{HS}^n}$

The boundary conditions are

$$\left.\frac{du^*}{dr^*}\right|_{r^*=0} = 0 \quad \text{and} \quad u^*|_{r^*=1} = 0 \tag{15}$$

The energy equation is written as

$$\rho c_p \frac{DT}{Dt} = \nabla.(k\nabla T) + \mu\Phi + s \tag{16}$$

where $\mu\Phi$ is the heat generation due to viscous dissipation and s is the Joule heating term given by E_x^2/σ where σ is the liquid resistivity given by [12] $\sigma = \frac{\sigma_0}{\cosh\left(\frac{ez\psi}{k_B T_{av}} \right)}$ where σ_0 is the electrical resistivity of neutral liquid.

The energy equation then becomes

$$(\rho c_p) u \frac{\partial T}{\partial x} = k\left(\frac{\partial^2 T}{\partial x^2} + \frac{1}{r}\frac{\partial}{\partial r}\left(r \frac{\partial T}{\partial r} \right) \right) + \mu_0 \left[\left(\frac{du}{dr} \right)^2 \right]^{\frac{n-1}{2}} \left(\frac{du}{dr} \right)^2 + \frac{E_x^2}{\sigma_0} \cosh\left(\frac{ez\psi}{k_B T_{av}} \right) \tag{17}$$

Let θ be the non-dimensional temperature defined as

$$\theta = \frac{T - T_w}{qH/k} \tag{18}$$

where $T_w$is the wall temperature and q is the wall heat flux.
For a constant heat flux condition,

iJETRM
International Journal of Engineering Technology Research & Management

$$\frac{\partial T}{\partial x}=\frac{dT_{\mathrm{w}}}{dx}=\frac{dT_{\mathrm{m}}}{dx} \tag{19}$$

so the axial conduction term disappears.

Equation (17) can be written as

$$(\rho c_{\mathrm{p}})u\frac{dT_{\mathrm{m}}}{dx}=k\left(\frac{1}{r}\frac{d}{dr}\left(r\frac{dT}{dr}\right)\right)+\ \mu_0\left[\left(\frac{du}{dr}\right)^2\right]^{\frac{n-1}{2}}\left(\frac{du}{dr}\right)^2+\frac{E_{\mathrm{x}}^2}{\sigma_0}\cosh\left(\frac{ez\psi}{k_{\mathrm{B}}T_{\mathrm{av}}}\right) \tag{20}$$

To determine $\frac{dT_{\mathrm{m}}}{dx}$ the above equation is integrated

$$\frac{dT_{\mathrm{m}}}{dx}=\frac{2\left(q+\int_0^R\left\{\mu_0\left[\left(\frac{du}{dr}\right)^2\right]^{\frac{n-1}{2}}\left(\frac{du}{dr}\right)^2+\frac{E_{\mathrm{x}}^2}{\sigma_0}\cosh\left(\frac{ez\psi}{k_{\mathrm{B}}T_{\mathrm{av}}}\right)\right\}dr\right)}{\rho c_{\mathrm{p}}u_{\mathrm{m}}R} \tag{21}$$

For steady fully-developed flow of power law fluid, Eq. (17) can finally be written as

$$\frac{d^2\theta}{dr^{*2}}+\frac{1}{r^*}\frac{d\theta}{dr^*}=2\left(1+SI_1+\frac{SS_{\mathrm{v}}}{K^2}I_2\right)\frac{u^*}{u_{\mathrm{m}}^*}-\frac{SS_{\mathrm{v}}}{K^2}N(r^*)\left(\frac{du^*}{dr^*}\right)^2-S\cosh\psi_{\mathrm{i}}^* \tag{22}$$

$$S_{\mathrm{v}}=\frac{\mu\sigma u_{\mathrm{HS}}^{n+1}}{E_{\mathrm{x}}^2\lambda_{\mathrm{D}}^2R^{n-1}}\ ,\ \ S=\frac{E_{\mathrm{x}}^2R}{q\sigma_0}\ \ ,u_{\mathrm{m}}^*=\int_0^1u^*dr^*\ \ ,\ I_1=\int_0^1\cosh\psi^*dr^*\ \ ,$$

$$I_2=\int_0^1N(r^*)\left(\frac{du^*}{dr^*}\right)^2dr^* \tag{23}$$

The boundary conditions are

$$\left.\frac{d\theta}{dr^*}\right|_{r^*=0}=0\ \ \text{and}\ \ \theta|_{r^*=1}=0 \tag{24}$$

The heat transfer rates are expressed in the form of Nusselt number which can be reduced to

$$Nu_\infty=\frac{hD_h}{k}=-\frac{2}{\theta_{\mathrm{m}}} \tag{25}$$

where θ_{m} is the bulk mean temperature of the fluid.

Equations (6), (15) and (21) are solved numerically using the tri-diagonal matrix algorithm. Central difference scheme is applied to the equations.

$$\psi_{i+1}^*\left(r_i{}^*+\frac{\Delta r^*}{2}\right)-\left(2r_i{}^*+K^2(\Delta r^*)^2r_i{}^*\Lambda_i^g\right)\psi_i^*+\psi_{i-1}^*\left(r_i{}^*-\frac{\Delta r^*}{2}\right)=0 \tag{26}$$

$$u_{i+1}^*\left(r_i{}^*+\frac{\Delta r^*}{2n}\right)-2r_i{}^*u_i^*+u_{i-1}^*\left(r_i{}^*-\frac{\Delta r^*}{2n}\right)=-\frac{(\Delta r^*r_i)}{nN_i^g}\left[\left(\frac{n+1}{n}\right)^n\Gamma+\frac{K^{n+1}}{n^n\zeta^*}\sinh\psi_i{}^*\right] \tag{27}$$

$$\theta_{i+1}\left(r_i{}^*+\frac{\Delta r^*}{2}\right)-2\theta_ir_i{}^*+\theta_{i-1}\left(r_i{}^*-\frac{\Delta r^*}{2}\right)=2(\Delta r^*)^2r_i{}^*\left(1+I_1S+I_2\frac{SS_{\mathrm{v}}}{K^2}\right)\frac{u_i^*}{u_m^*}-\frac{SS_{\mathrm{v}}}{4K^2}r_i{}^*N_i(u_{i+1}^*-u_{i-1}^*)^2-S(\Delta r^*)^2r_i{}^*\cosh\psi_i{}^* \tag{28}$$

$\Lambda_i^g=\frac{\sinh\ \psi_i^*}{\psi_i^*}$ and N_i^g change the non-linear system of governing equations into linear system of difference equations. These values are set after each iteration till the error obtained in the order of 10^{-8}. To evaluate the integrals Trapezoidal method is used.

Results and Discussion

The above discretized equations were solved and the results obtained are discussed in this section. To verify the accuracy of the method used, the values of the parameters were set in such a manner that the equations represent macroscale flow of a Newtonian fluid through a tube without viscous dissipation and the effect of the potential variation is negligible. The values set were $\Gamma=1\times10^5$, S=0, S_{v}=0, n =1, ζ^*=0. The value of Nusselt number obtained was 4.36027 which is close to the analytical value 4.36.

ISSN: 2456-9348
Vol (01) _Issue (04) Impact Factor: 4.520

International Journal of Engineering Technology Research & Management

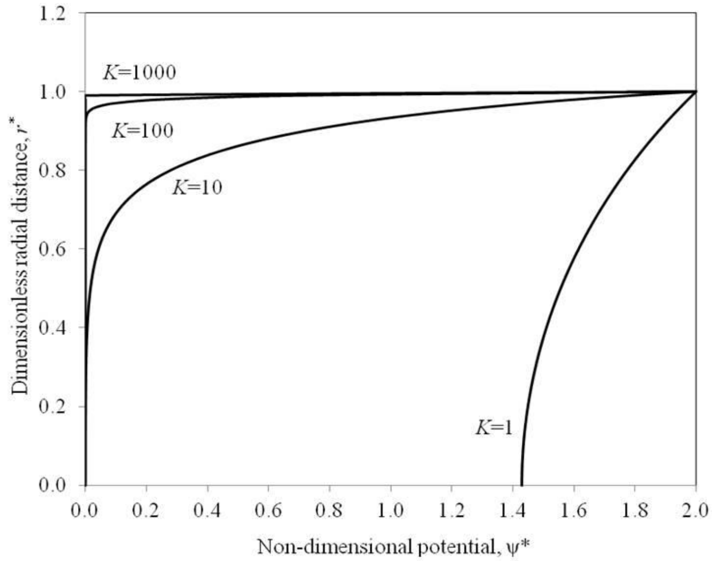

Fig1.2 Potential distribution for various values of K when ζ^*=2.

The potential distribution is plotted in Fig. 2 at *K*=1,10,100,1000 when ζ^*=2. It is clearly seen that the effect of the potential distribution is present only at small values of *K*, i.e. when *K*<100. Below *K*=10, the EDL interact about the channel axis.

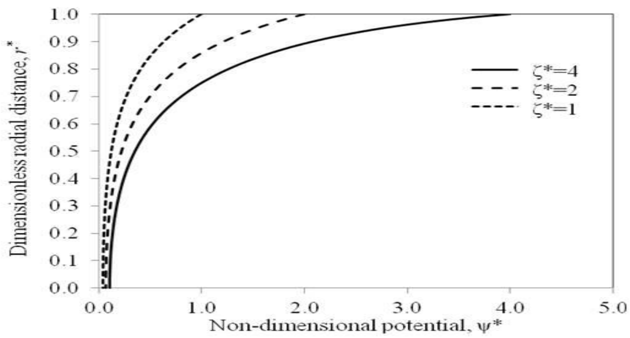

Fig.1.3 Variation in potential distribution at various values of non-dimensional zeta potential when K=5.

In Fig. 3, the effect of non-dimensionalised zeta potential on the potential distribution at *K*=5 is shown. This shows that, higher the value of ζ^*, more pronounced is the effect of zeta potential on the potential profile.

iJETRM
International Journal of Engineering Technology Research & Management

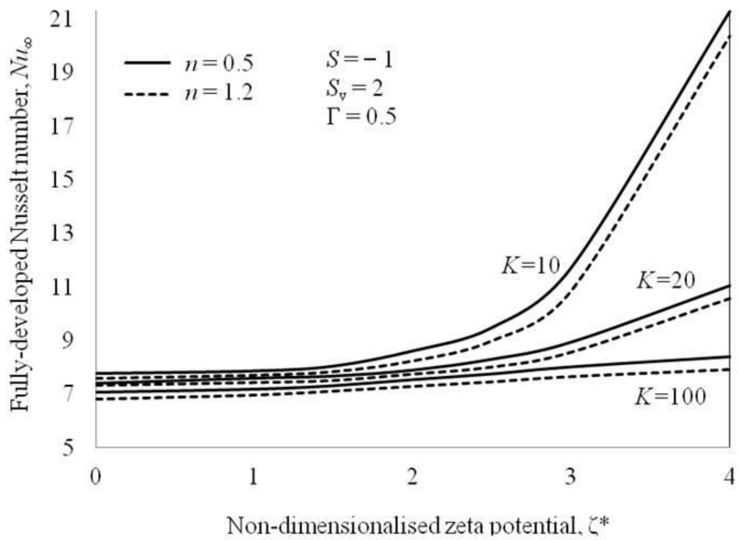

Fig.1.4 Effect of dimensionless zeta potential, ζ*, on fully-developed Nusselt number at different values of Debye Hückel parameter, K, and flow behaviour index, n.

The effect of non dimensional zeta potential on Nusselt number at various values of *K* is seen in Fig. 4. As the value of *K* is lowered, the curves become increasingly steep after $\zeta^*=2$. This behavior is expected as the effect of the EDL depreciates rapidly when *K* is increased, and loses its capacity to change the rate of Joule heating.

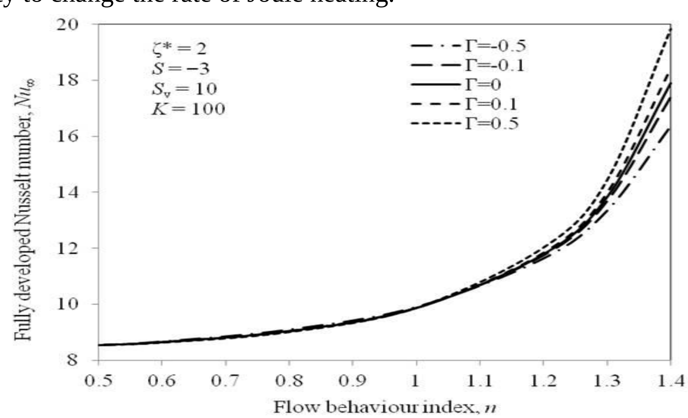

Fig.1.5 Variation of fully-developed Nusselt number with n at various values of velocity scale ratio, Γ.

Figure 5 illustrates the variation of Nusselt number with flow behaviour index, *n*, at various values of velocity scale ratio, Γ. It is seen that at higher values of *n*, (higher than *n*=1.41) the fully-developed Nusselt number, Nu_∞, seems to rapidly decrease. Such a

iJETRM
International Journal of Engineering Technology Research & Management

discrepancy was not found in the analysis conducted by Babaie et al. for microchannels. It is observed that when the ratio of viscous dissipation to Joule heating increases beyond a particular value, Nu_∞, shows a sudden decline. This value varies with n and Γ, though Γ is absent in the governing equation of temperature profile. This is possible, because the value of Γ changes the velocity profile, which in turn affects the temperature profile and Nu_∞. The velocity profile in such cases show a very high value of mean non-dimensional velocity.

CONCLUSION

The thermal transport characteristics of a combined electroosmotic and pressure driven flow of power-law fluids in a microtube was studied. The electrical, momentum and energy equations were solved numerically for fully developed flow condition. The effect of viscous dissipation and Joule heating were considered. From the above numerical analysis carried out to study the effect of the various governing parameters on the Nusselt number, the following conclusions are drawn:

- The effect of the electric double layer and hence the zeta potential is appreciable only when the value of the Debye-Hückel parameter is less than 100.
- The effect of the EDL increases in prominence when the zeta potential is increased.
- When the velocity scale ratio, Γ, is increased the Nusselt number increases. Positive values of Γ result in higher Nusselt number than the negative values.
- The effect of flow behavior index, n, plays a major role in the heat transfer characteristics at lower values of Debye- Hückel parameter.
- Viscous dissipation, which can be neglected for purely electroosmotic flow, becomes a influencing parameter in combined electroosmotic and pressure-driven flow.

REFERENCES

[1] Sobhan, C.B., & Peterson, G.P. (2008). Microscale and Nanoscale Heat Transfer, CRC Press (Taylor & Francis).
[2] Reuss, F.F. (1809). Charge induced flow, *Proc. Imperial Soc. Naturalists Moscow*, **3**, 327-344.
[3] Burgreen D., & Nakache, F.R. (1964). Electrokinetic flow in ultrafine capillary slits, *J. Phys. Chem.*, **68**, 1084-1091.
[4] Rice, C.L., & Whitehead, R. (1965). Electrokinetic flow is narrow cylindrical capillary, *J. Phys. Chem.*, **69**, 4017-4024.
[5] Arulanandam, S., & Li, D. (2000). Liquid transport in rectangular microchannels by electroosmotic pumping, *Colloids Surf. A*, **161**, 89-102.
[6] Xuan, X., & Li, D. (2005). Electroosmotic flow in microchannels with arbitrary geometry and arbitrary distribution of wall charge, *J. Colloid Interf. Sci.*, **289**, 291-303.
[7] Mayens, D., & Webb, B.W. (2003). Fully-developed electroosmotic heat transfer in microchannels, *Int. J. Heat Mass Transfer*, **46**, 1359-1369.
[8] Liechty, B.C., Webb, B.W., &Maynes, R.D., (2005). Convective heat transfer characteristics of electro-osmotically generated flow in microtubes at high wall potential, *Int. J. Heat Mass Transfer*, **48**, 2360-2371.

iJETRM
International Journal of Engineering Technology Research & Management

[9] Zhao, C., Zholkovskij, E., Masliyah, J.H., & Yang, C. (2008). Analysis of electroosmotic flow of power-law fluids in a slit microchannel, *J. Colloid Interface Sci.*, **326**, 503-510.
[10] Probstein, R.F. (1994). Physiochemical Hydrodynamics, 2nd edition, Wiley, New York.
[11] Yang, C., Li, D., &Masliyah, J.H. (1998). Modeling forced liquid convection in rectangular microchannels with electrokinetic effects, *Int. J. Heat Mass Transfer*, **41**, 4229-4249.
[12] Sadeghi, A., Yavari, H., Saidi, M.H., & Chakraborty, S. (2011). Mixed electroosmotically and pressure-driven flow with temperature-dependant properties, *J. Thermophys. Heat Transfer*, **25**, 432-442.